MATERIAL PROPERTIES

Flow curve approximation of high-strength aluminium alloys in heat-assisted forming processes

M. Schmiedt[1] · R. Schneider[2] · J. Jung[1] · W. Rimkus[1] · A. K. M. De Silva[3]

Abstract

Predicting the flow behaviour at high strain values beyond uniform elongation is a critical factor in sheet metal forming, especially in the context of heat-assisted forming processes of lightweight materials. Based on uniaxial tensile tests conducted at the temperature profiles of the Hotforming, W-Temper, and Warmforming process routes this study presents the determination of the flow curve for EN AW-7021 sheet material using five commonly used empirical approximation models. A support point obtained from layer compression tests was introduced to analyse the accuracy of the extrapolation models at higher strain values. All models considered were found to be in good agreement with the experimental tensile test data in the area of uniform elongation. However, the empirical approximation models show significant differences in strain hardening behaviour when higher strain values and varying temperature profiles are considered. For the Hotforming and W-Temper process routes, the Hockett-Sherby model estimates the flow behaviour with the highest accuracy. When using the Warmforming process, all approximation models considered seem to estimate the flow behaviour with reasonable accuracy, however the Ludwik-Hollomon modified equation shows the best correlation with the experimental data.

Keywords Aluminium · Mechanical testing · Flow curve · Forming process

1 Introduction

A widely used method of lightweight construction is the use of high-strength aluminium alloys due to their advantageous strength-to-weight ratio. In the automotive or aerospace industries, the substitution of steel alloys with such lightweight materials is a means of reducing the nominal component weights [1, 2]. Although for most automotive panel applications 5000 and 6000 series Al alloys are currently used, the potential use of high-strength aluminium alloys for structural components is growing rapidly. In the aerospace industry, 7000 and 2000 series alloys are used primarily because of their high strength and good corrosion resistance [3]. Most of these aluminium parts are manufactured by forming, but the formability of certain aluminium alloys, such as the 7000 series, is limited at room temperature. To improve the forming behaviour, various heat-assisted processes have been investigated such as Hotforming [4], W-Temper [5], or the Warmforming [6] process routes.

The prediction of local plastic strains is a critical factor for process and tool design in sheet metal forming. Flow curves are used to accurately model these processes in a finite element method (FEM) simulation as they indicate strain hardening up to the maximum equivalent strain values. It is worth noting that most FEM software assumes a monotonic increasing curve to model forming processes [7]. Zhuang et al. [8] discussed three options for obtaining such data: experimental, analytical, and numerical methods. Commonly used experimental methods for determining the flow curve of sheet metals include tensile tests [9], bulge tests [10], shear tests [11], plain strain compression tests [12], and layer compression tests [13]; the latter being a modification of the plain strain compression test to meet the operating conditions of sheet metal forming processes. Merklein and Kuppert [14] demonstrated that the flow curves obtained from layer compression tests show a high correlation with those from uniaxial tensile tests when special

✉ M. Schmiedt
  michael.schmiedt@hs-aalen.de

1 Lightweight Technology Centre, Aalen University, Beethovenstraße 1, 73430 Aalen, Germany

2 University of Applied Sciences Ulm, Prittwitzstraße 10, 89075 Ulm, Germany

3 Glasgow Caledonian University, Cowcaddens Road, Glasgow G4 0BA, UK

attention is paid towards the reduction of friction between the specimen and the test equipment. In addition, the layer compression test provides flow curves with higher strain values as no necking occurs. However, the most common method of obtaining flow curves is the uniaxial tensile test, where the experimental data are extrapolated to true strain values of $\varepsilon \geq 1$. Analytical methods are based on formulations that describe the flow curve by physical or mathematical equations, as demonstrated by Albiez et al. [15] for the aluminium alloy EN AW-6016. Although analytical extrapolation methods are time and cost-effective, Gese et al. [16] demonstrated potential inaccuracies in terms of the choice of the approximation model and the experimental data used for extrapolation. In addition to analytical approaches, finite element analysis (FEA) can be used to numerically estimate the flow behaviour at high strain values. By using this approach, as presented by Joun et al. [17], an iterative scheme based on the local deformation behaviour in the necking region is applied to minimise the error between the measured and predicted load-strain curves.

However, for the aluminium alloy EN AW-7021, there are limited studies about the flow behaviour during heat-assisted forming processes. This study presents the determination of the flow curve for EN AW-7021 sheet material by analytical approximation models using experimentally obtained stress-strain data. Tensile tests and layer compression tests with the corresponding temperature profiles of the Hotforming, W-Temper and Warmforming process routes are carried out to analyse the accuracy of five commonly used analytical extrapolation models at higher strain values.

2 Theoretical and experimental background

2.1 Flow curve determination

It is well known from the literature how to convert experimentally determined engineering stress (σ_0) and engineering strain (e) data into true stress (σ) and true strain (ε) diagrams [18]. Analytical modelling and extrapolation of flow curves can be achieved using physically based (internal variable), semi-empirical, or empirical material models [19]. A major advantage of internal variable models is their realistic description of the flow behaviour beyond the uniform elongation region. However, the physical nature of such models results in complex systems of differential equations with a high number of parameters, as shown by Svyetlichnyy [20]. From an application point of view, it may be reasonable to describe the flow behaviour by mathematical equations based on empirical constants. Some of the commonly used empirical models are listed in Table 1.

The Ludwik-Hollomon and Ghosh equations are power law approximations that exhibit relatively high strain

Table 1 Empirical models for the extrapolation of flow curves [21]

Empirical model	Equation	
Ludwik-Hollomon	$\sigma = A * \varepsilon^n$	(Eq. 1)
Ludwik-Hollomon modified	$\sigma = A * \varepsilon^{n+R}$	(Eq. 2)
Ghosh	$\sigma = A * (B + \varepsilon)^n - C$	(Eq. 3)
Hockett-Sherby	$\sigma = \sigma_s - (\sigma_s - \sigma_y) * exp(-D * \varepsilon^E)$	(Eq. 4)
Voce	$\sigma = \sigma_s - (\sigma_s - \sigma_y) * exp(-F * \varepsilon)$	(Eq. 5)

hardening along the true stress (σ) and true strain (ε) curve. The Ghosh equation extends the well-known Swift model by introducing a free parameter C. It is used to further adjust the hardening behaviour and thus describe the flow behaviour with higher accuracy. Deviations between the approximated and observed flow behaviour should be expected as the strain hardening exponent (n) and thus, the strength coefficient (A) varies with deformation but is assumed to be constant here. It should also be noted that when using the Ludwik-Hollomon equations with an epsilon value of zero, the stress value will be zero and therefore the slope of the flow curve approaches infinity which does not correspond to reality. Both modelling approaches are capable of describing the typical hardening behaviour of particularly low-alloy steels in the uniform elongation region. However, the flow behaviour may not be described with sufficient accuracy at higher strain values or when using high-strength steels and aluminium alloys [22]. The Hockett-Sherby and Voce exponential equations include the yield strength (σ_y) and saturation stress (σ_s) to account for dynamic recovery mechanisms during deformation. The saturation stress, originally intended to be a physical value, is defined empirically to approximate the flow curve for small deformation values and to flatten the curve for high deformation values [22]. The free parameters B, C, D, E, F and R are defined as constants. The Voce equation was examined for extrapolating various steel grades, nickel alloys and titanium alloys [23], but is typically used to describe the flow behaviour of aluminium alloys [24]. For tailor heat treated aluminium blanks, the Hockett-Sherby equation was found to show the highest correlation with the experimental tensile test data [25].

2.2 Layer compression tests

Depending on the empirical approximation model used (Table 1), flow curve formulations may lose accuracy and deviate from the experimentally obtained data when extrapolated to strain values beyond the uniform elongation region. To verify this deviation and hence the prediction error layer compression tests, also referred to as stack compression tests, are carried out to evaluate the flow behaviour up to relatively high strain values. The test

uses circular pieces which are stacked to form a cylindrical specimen and then uniaxially compressed in the direction of the sheet thickness. As the testing procedure is not yet standardised it is based on the standard compression test according to DIN 50106 [12]. The most comprehensive work in this area was conducted by Merklein and Kuppert who presented a method for evaluating the layer compression test on anisotropic materials [14, 26]. Alves et al. [13] demonstrated that the results of the layer compression test are nearly identical to those obtained by the standard compression test using solid specimens. Special attention must be paid to the relative orientation (rolling direction) of the discs and the friction between the specimen and test equipment as this not only affects the uniaxial stress state but also causes slippage between the individual layers. The usage of solid lubricants, such as Teflon, has proven to be effective [27].

The extrapolation of the flow curve obtained from tensile tests is compared to a support point based on layer compression tests (Fig. 1). The deviation $\Delta\sigma$ from the support point can be used to identify models capable of accurately approximating the flow behaviour beyond uniform elongation.

Based on the standard compression test, the values of true stress (σ) and true strain (ε) for the layer compression test are determined using Eqs. 6 and 7 [26].

$$\sigma = \frac{F * h}{A_0 * h_0} \tag{6}$$

$$\varepsilon = ln\left(\frac{h}{h_0}\right) \tag{7}$$

The applied force is denoted by F, A_0 is the initial specimen area, h is the specimen height during the test and h_0 is the initial specimen height. Both equations are based on the height reduction measured by the crosshead movement of the testing machine.

3 Experimental setup

In order to determine the flow curve in the uniform elongation region uniaxial tensile tests are carried out in accordance with DIN EN ISO 6892 [9] on EN AW-7021-T6 sheet material using a universal testing machine (Zwick Z100). According to DIN 50125 [28] tensile specimens (geometry H) were manufactured with a parallel length of 75 mm and a thickness of 2 mm and tested at a crosshead speed of 5 mm/min, resulting in a strain rate of $\dot{\varepsilon} = 0.0017$ s^{-1}. Special attention was given to the temperature profiles (Hotforming, W-Temper and Warmforming, Fig. 4) throughout the test
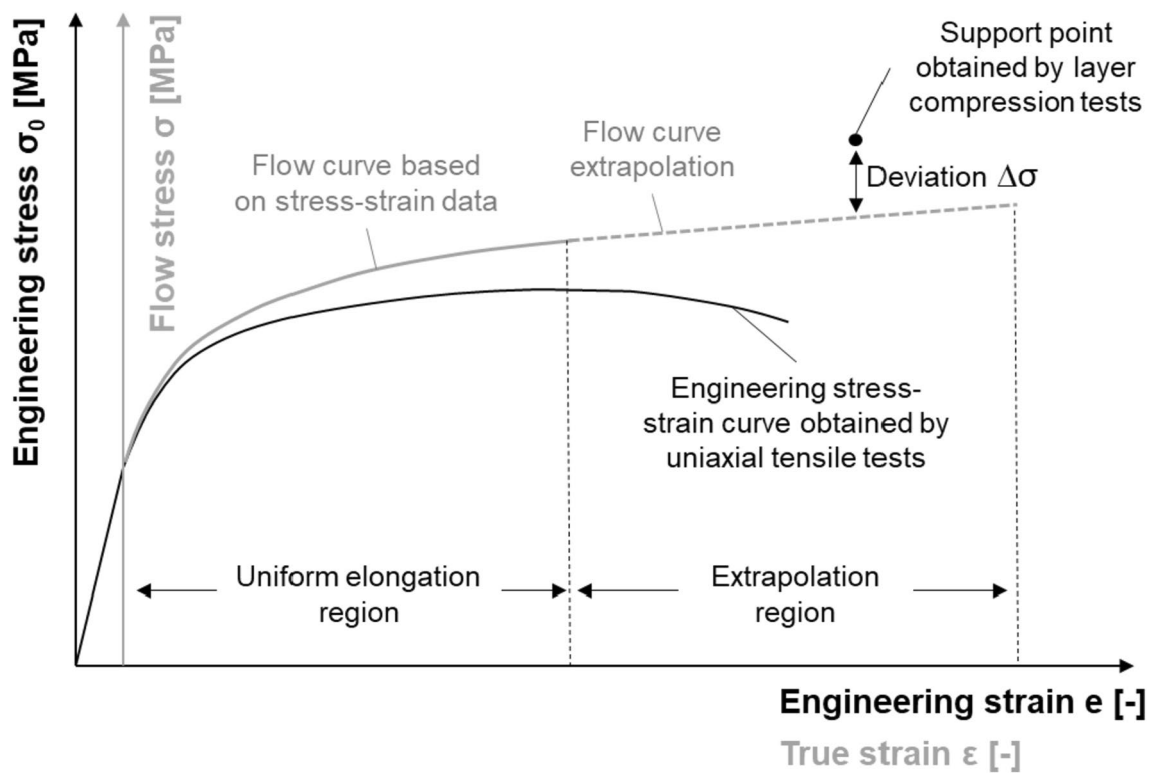

Fig. 1 Comparison between the approximated flow curve and the support point

series. A radiation furnace next to the testing machine (Hotforming, W-Temper) and a radiation furnace mounted on the universal testing machine (Warmforming, Fig. 2) were used to achieve the required temperature profile.

For each temperature profile and rolling direction r (longitudinal 0r, transverse 90r and 45-degree angle 45r) five tensile tests were carried out and averaged to provide a significant database for flow curve approximation. The method of least square error (LSE) was used to determine the coefficients defined in Table 1 (GRG nonlinear solver function in MS Excel 2019) and to minimise the deviation between the experimental tensile test data in the uniform elongation region and the approximation model. The derived flow curve was then extrapolated to the true strain value of $\varepsilon = 1$.

For layer compression testing square plates with an edge length of 8 mm were cut from the same sheet material as for the tensile test (EN AW-7021-T6, thickness 2 mm) and laminated using a two-component epoxy resin adhesive. All plates were oriented in the same rolling direction and the outer surface of the stack was turned to a diameter of 6 mm. Special attention was given to an aspect ratio of $h_0/d_0 = 1$ (where h_0 represents the initial height and d_0 is the initial diameter of the specimen) to ensure compliance with the standard compression test for solid cylindrical specimens which specifies a ratio of $1 \leq h_0/d_0 \leq 2$ to avoid bending or buckling [12]. The tests were carried out using a universal testing machine (Zwick Z100) between two parallel compression plates. To reduce friction between the compression plates and the specimen the tool surfaces were polished and a Teflon film was applied. The initial height and diameter of the specimen were measured using a micrometre. The

height of the specimen after testing was determined by the crosshead displacement of the testing machine with elastic deformation being compensated by a correction curve. The correction curve was measured prior to testing and indicates the deformation of the machinery and test equipment as a function of the force applied. The support point was determined by reducing the initial height of the test cylinder to approximately 50% and 60%. An external radiation furnace (for Hotforming and W-Temper) next to the universal testing machine and a heating sleeve mounted on the compression plates (for Warmforming, Fig. 3) was used to apply the process-oriented temperature profile (Fig. 4) to the specimens. As with the tensile tests the crosshead speed was set at 5 mm/min and five layer compression tests were carried out at each temperature profile. Figure 3 shows the specimen preparation and the schematic setup of the layer compression test.

To characterise the temperature profile tensile and layer compression specimens were fitted with thermocouples to monitor the temperature values at a frequency of 5 Hz. Measurements were taken for the external radiation furnace (Linn ET-LM 312.07) and the heating devices (Maytec HTO-23, HASCO H1134) mounted on the universal testing machine. Each heating curve in Fig. 4 is averaged over three measurements.

In the Hotforming process, the specimen is heated in a separate furnace to the solution annealing temperature of approximately 515°C Fig. 4, point 1) and held for a minimum of 5 minutes (point 2). The specimen was then transferred to the universal testing machine (point 3), where it was held between the cold compression plates (layer
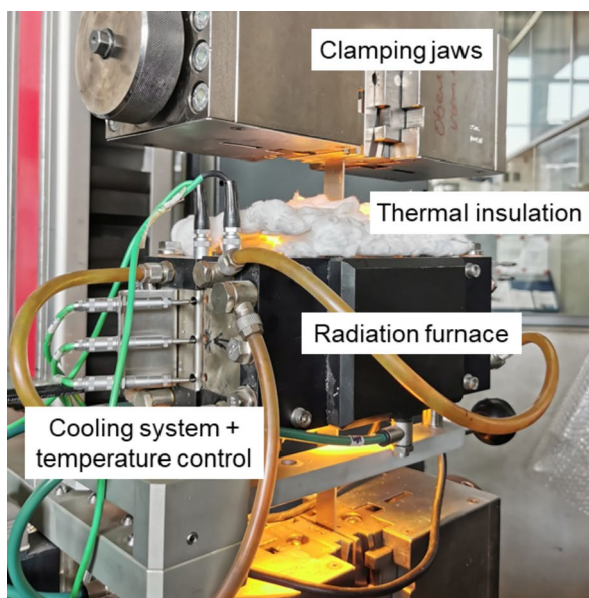

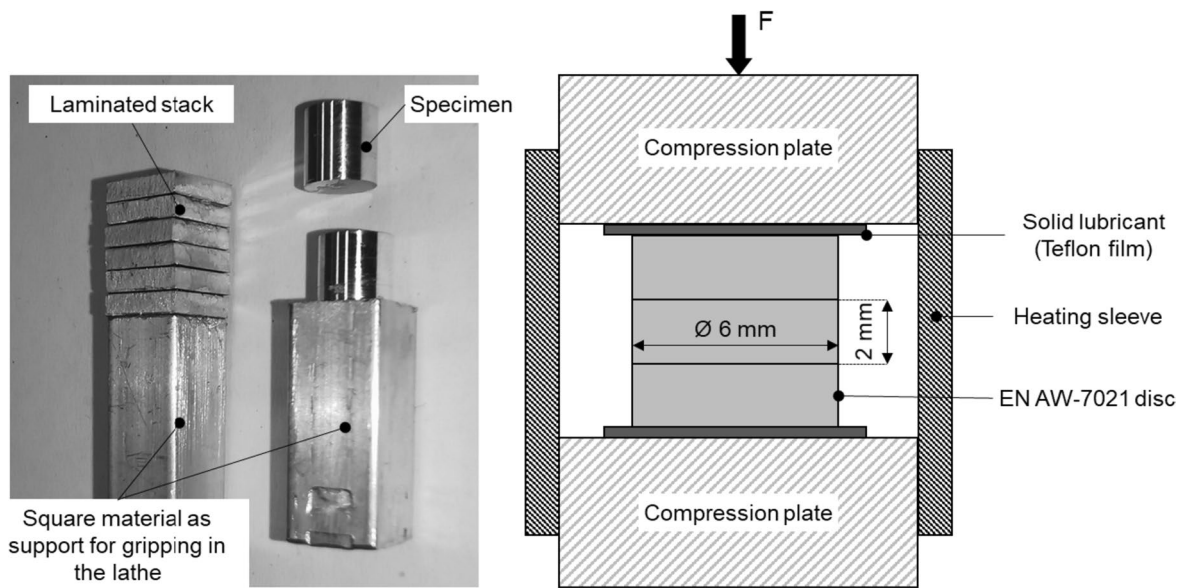**Fig. 2** Tensile test setup with heating devices

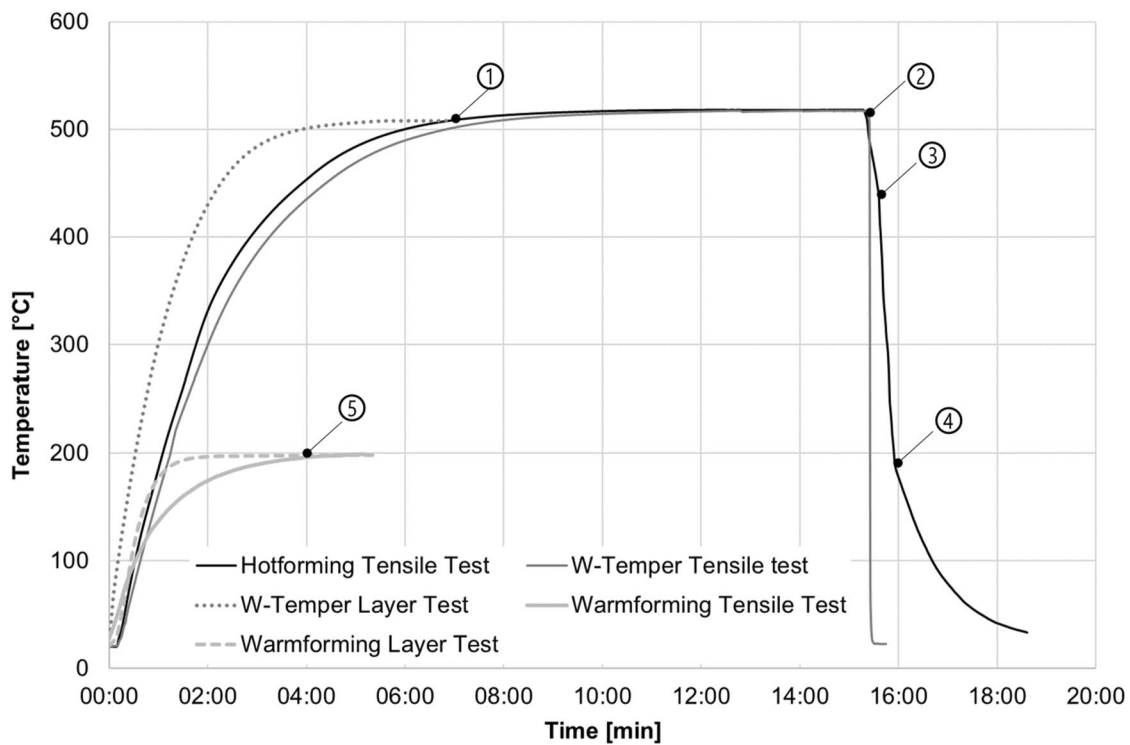**Fig. 3** Layer compression test setup and specimen preparation

Fig. 4 Temperature profile of the Hotforming, W-Temper and Warmforming process

compression test) or between the cold clamping jaws and quenched with compressed air during testing (tensile test). When using an EN AW-7021 alloy the temperature of the specimen must not fall below 380°C during transfer from the furnace to the universal testing machine as precipitation reactions start when cooling below this temperature.

The critical cooling rate for EN AW-7021 is approximately 10 K/s and should be kept below 200°C (point 4) to avoid quench induced precipitation or loss of age hardening potential [29]. For the W-Temper process, which is a thermally decoupled forming process, the specimen is heated in a separated furnace, held at a solution annealing temperature of

approximately 515°C and then quenched. In this test series, quenching was carried out using a water bath. The cold specimen was tested at ambient temperature within 30 min before the onset of natural ageing of the material [24]. The dotted line in Fig. 4 illustrates the heating behaviour of the layer compression specimens in the external furnace.

For Warmforming the specimens are heated, held at approximately 200°C and then tested isothermally. For the tensile test, a radiation furnace was mounted on the universal testing machine and closed around the positioned tensile specimen. A heating time of 4 minutes was measured to reach the required temperature (point 5). For the layer compression tests the compression plates were heated to approximately 200°C using a heating sleeve and the specimens were heated by direct contact (dashed curve).

4 Results and discussion

Figure 5 shows the flow curves of EN AW-7021 material for different temperature profiles (average of five tests each). Further, flow curves tested in the longitudinal direction (0r) are shown as no significant changes in the true stress-strain behaviour were observed with varying rolling directions. Both the strain hardening behaviour and the onset of yielding are nearly identical; for Hotforming 101.8 ± 6.2 MPa

and W-Temper 99.5 ± 4.7 MPa. The highest uniform elongation values were obtained by applying the W-Temper process route (up to $\varepsilon = 0.23$). In accordance with the results of Schneider et al. [30] the serration of the true stress values is due to the Portevin-Le Chatelier (PLC) effect. The curve characteristics correspond well with the results from Grohmann [31] where flow curves were obtained for the W-Temper forming of AMAG 7021 sheet material. Tensile tests carried out at a temperature of 200°C (Warmforming) indicate an increased onset of yielding (320.9 ± 7.5 MPa) but the material exhibits softening behaviour (negative strain hardening coefficient). The dashed curve shows the flow behaviour of the Warmforming testing procedure beyond uniform elongation (true strain values of up to $\varepsilon = 0.02$). This behaviour corresponds well with the stress values obtained by Polak et al. for EN AW-7075 at elevated temperatures [6].

The flow curves obtained from the layer compression tests are depicted by dotted lines in Fig. 5. To enhance comparability with the tensile test results, the flow curves are shown up to a strain value of $\varepsilon = 0.3$. For the W-Temper process route, the flow curves obtained from tensile and layer compression tests are almost identical (with a maximum deviation of 6 MPa) and the shape of the compressed specimen remains cylindrical, indicating a negligible influence of friction. When considering the Hotforming process, the maximum deviation increases to 17 MPa and the specimen
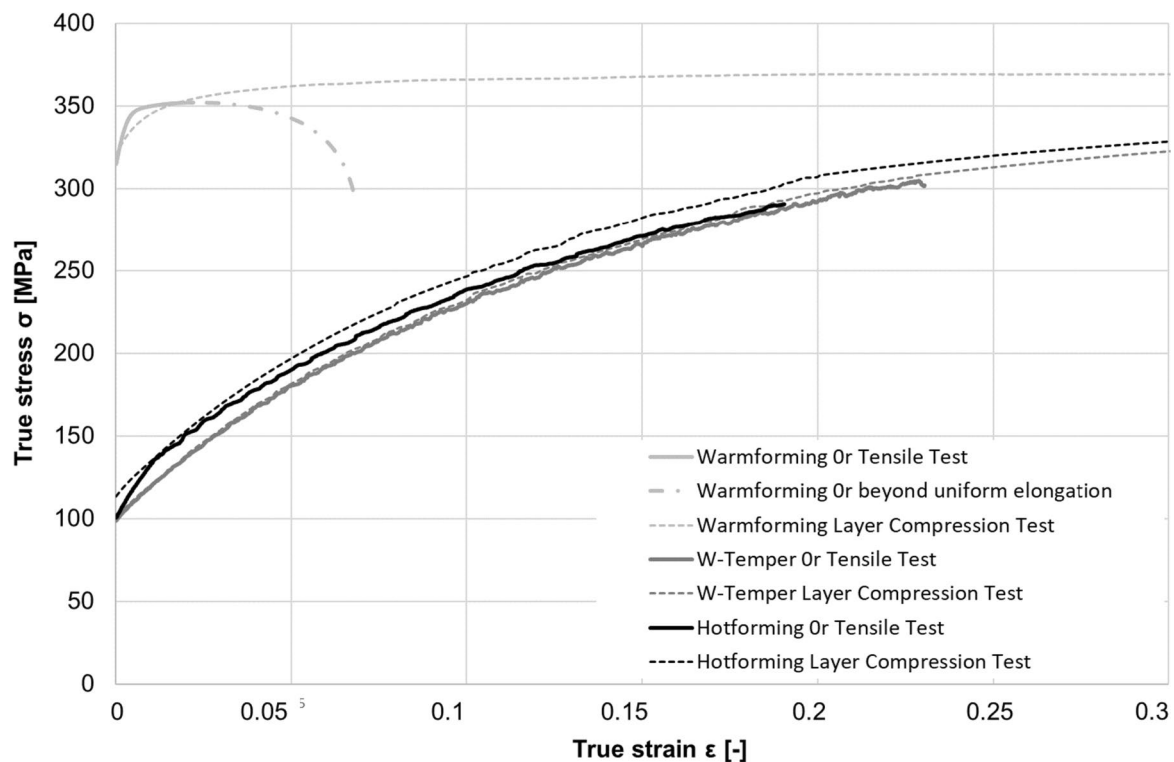

Fig. 5 Flow curves of EN AW-7021 sheet material for different temperature profiles

exhibit a bulged geometry after testing. One reason for this can be found in the altered frictional conditions caused by the applied temperature profile. When positioned in the compression plates and thus on the Teflon film, the specimen has a temperature of approximately 430°C (Fig. 4), which means that the solid lubricant is subjected to short-term heating. Compared with the W-Temper or Hotforming process routes, the deviation of the flow curves is most significant for Warmforming with a maximum stress difference of 19 MPa. The flatter flow curve obtained from the layer compression test suggests that the deformation behaviour is influenced by the epoxy resin adhesive used for laminating of the specimens. This influence is not discernible in the W-Temper and Hotforming processes due to the solution heat treatment prior to forming. For the Hotforming process, future work ought to address on the reduction of the friction influence by using heat resistant lubricants or compensate frictional force with factors as suggested by Lenzen et al [32]. When considering the Warmforming route, further investigations should be carried out on the modification of the heated test equipment to enable the use of digital image correlation systems for sample measurement.

For accurate comparison between layer compression and tensile test data, it is essential to assume isotropic forming behaviour, i.e. equal deformation in the tangential and radial directions. For highly anisotropic materials, the axes in and perpendicular to the rolling direction must be analysed and the data mathematically converted as a function of the prevailing major strain values [14]. The optical measuring system ZEISS Axio Zoom.V16 was used to measure the diameters of the compressed middle plate at 0° and 90° to the rolling direction. Figure 6 compares the biaxial Lankford coefficients for each process route. The values correspond well with the results from Hetz et al. [33], in which a single layer compression test was used for determining the biaxial Lankford coefficient. The results showed a coefficient close to 1.0 for EN AW-7020-T6 sheet material, indicating isotropic material behaviour when a Teflon film is used as a lubricant.

Since the biaxial anisotropy values for each process are approximately equal to 1, an isotropic forming behaviour is assumed. Table 2 summarises the results of the layer compression testing as a function of the process-related temperature profiles (average of five tests each). The stress values at a height reduction of 50% are nearly identical if the Hotforming (358.8 ± 10.2 MPa) and W-Temper (348.4 ± 3.9 MPa) process routes are compared. With a height reduction of 60% the stress values increase to 364.6 ± 9.1 MPa (Hotforming) and 355.1 ± 2.8 MPa (W-Temper). Considering the Warmforming process route, flow curve determination is possible

Table 2 Support points obtained from layer compression tests for EN AW-7021 sheet material

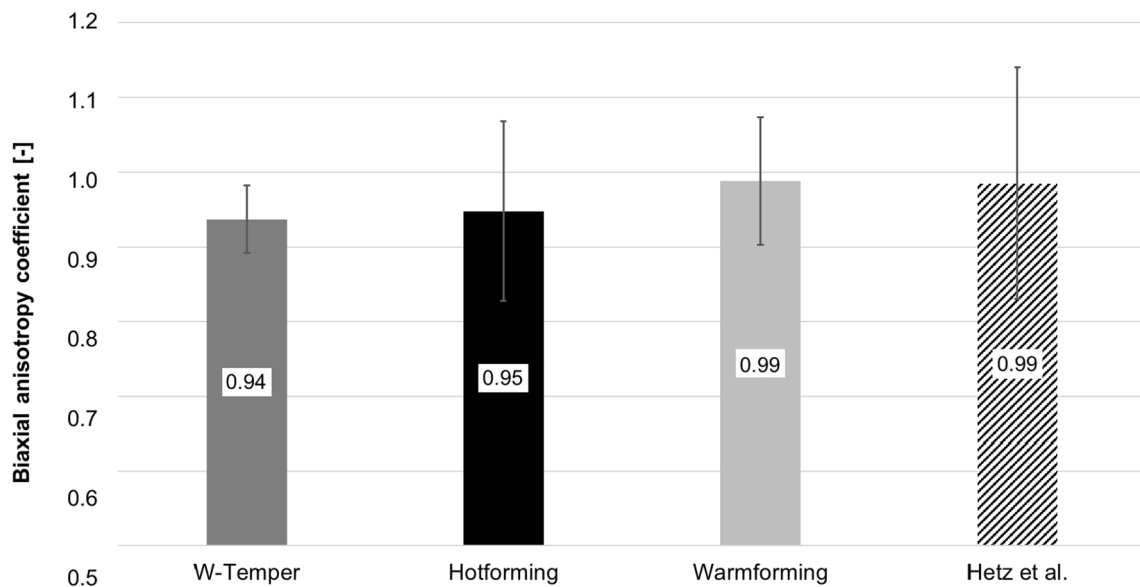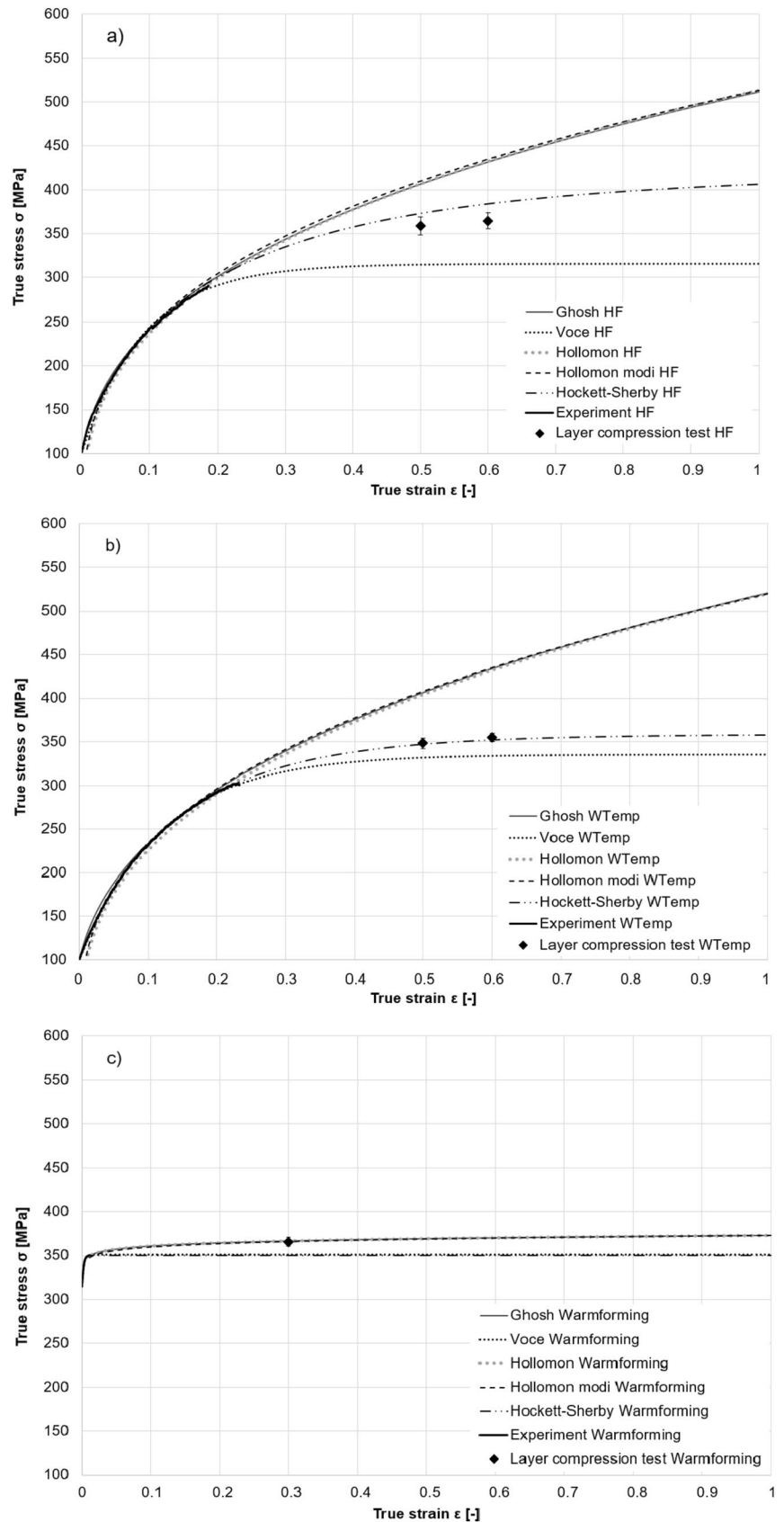| Process	h_0 [mm]	A_0 [mm^2]	$\sigma(\varepsilon = 0.3)$ [MPa]	$\sigma(\varepsilon = 0.5)$ [MPa]	$\sigma(\varepsilon = 0.6)$ [MPa]
Hotforming	6.11	28.18	–	358.8 ± 10.2	364.6 ± 9.1
W-Temper	6.06	28.08	–	348.4 ± 3.9	355.1 ± 2.8
Warmforming	6.07	28.11	365.9 ± 2.9	–	–

Fig. 6 Biaxial anisotropy coefficients for different temperature profiles

Fig. 7 Approximated flow curves of EN AW-7021 sheet material as a function of the **a** Hotforming (HF), **b** W-Temper (WTemp), and **c** Warmforming temperature profile

for strain values of approximately 30% as the specimens fail at higher strains.

Figure 7a–c show the experimentally determined flow curves, the approximation models and the support points of the EN AW-7021 sheet material as a function of the forming process used. Table 3 shows the coefficients of the extrapolation formulas used. The least squares error (LSE) is given as a measure of the correlation between the experimental and the approximated data in the uniform elongation region. Figure 8 shows the evaluated deviation between the measured and predicted flow stress values for different approximation models and temperature profiles.

Considering the deviation for EN AW-7021 material (Fig. 8) when Hotforming is applied, it can be seen that the flow stress values calculated using the Voce equation differ from the experimentally determined data by approximately 44 MPa (12%) at 50% true strain and 49 MPa (14%) at 60% true strain. The stress values determined using the Ludwik-Hollomon equation differ by approximately 48 MPa (13%) at 50% true strain and 68 MPa (19%) at 60% true strain. When using the Ludwik-Hollomon-modified model the LSE in the uniform elongation region can be significantly reduced from 20.17 to 4.72 MPa (Table 3) but without improving the deviation error in the extrapolation region. Using the Hockett-Sherby equation a deviation between the measured

Table 3 Coefficients of flow curve extrapolation models for EN AW-7021: a) Hotforming, b) W-Temper and c) Warmforming

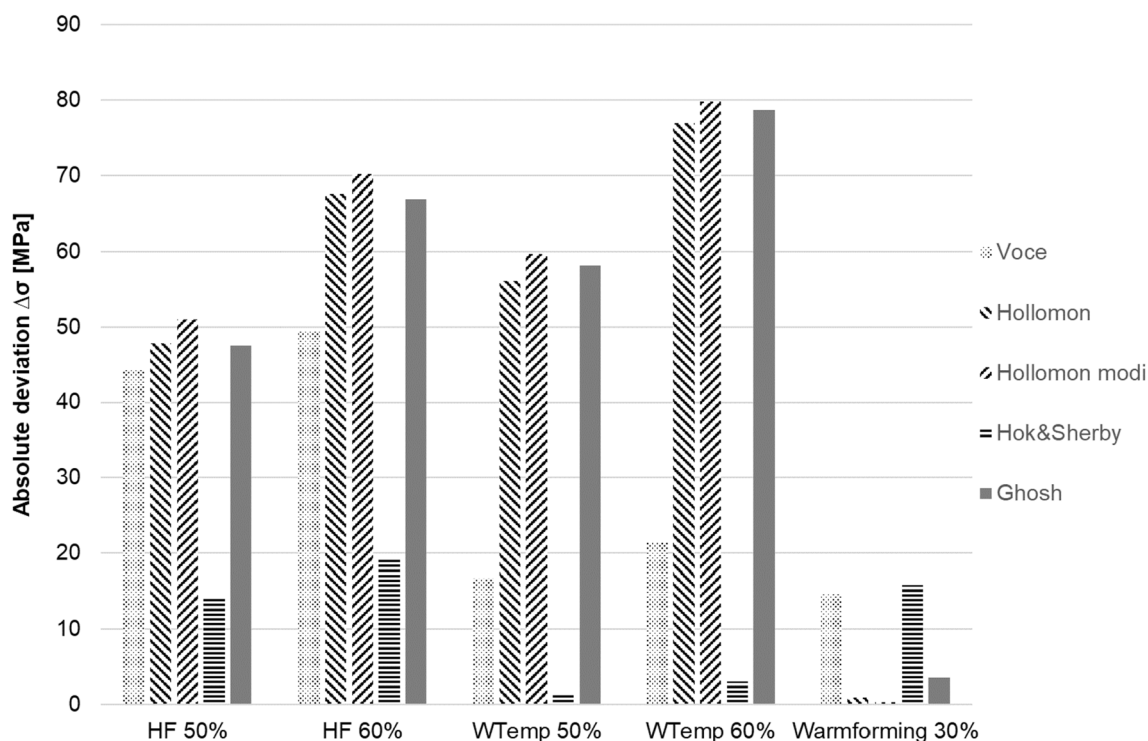| Coefficient	Hollomon	Hollomon modified	Ghosh	Hockett-Sherby	Voce
(a) Hotforming process					
n	0.33	0.33	0.33	–	–
A	510.28	510.28	510.28	–	–
R	–	− 0.0110	–	–	–
B	–	–	0.0082	–	–
C	–	–	0.20	–	–
D	–	–	–	3.75	–
E	–	–	–	0.78	–
F	–	–	–	–	10.98
σ_s	–	–	–	426.93	315.58
σ_y	–	–	–	101.83	101.83
LSE	20.17	4.72	7.93	1.47	3.61
(b) W-Temper process					
n	0.36	0.36	0.36	–	–
A	518.97	518.97	518.97	–	–
R	–	− 0.0128	–	–	–
B	–	–	0.0105	–	–
C	–	–	0.12	–	–
D	–	–	–	6.02	–
E	–	–	–	0.92	–
F	–	–	–	–	8.37
σ_s	–	–	–	358.45	335.32
σ_y	–	–	–	99.49	99.49
LSE	11.03	7.83	13.78	1.46	1.91
(c) Warmforming process					
n	0.0146	0.0146	0.0146	–	–
A	373.22	373.22	373.22	–	–
R	–	0.0013	–	–	–
B	–	–	2.38 E-05	–	–
C	–	–	0.0226	–	–
D	–	–	–	984.87	–
E	–	–	–	1.15	–
F	–	–	–	–	375.07
σ_s	–	–	–	350.06	351.12
σ_y	–	–	–	315.20	314.91
LSE	5.85	5.64	5.86	0.24	0.57

Fig. 8 Deviation of the approximation models from the support point as a function of the forming process and strain value

and calculated flow curves of 15 MPa (4%) at 50% true strain and 20 MPa (5%) at 60% true strain can be observed. The average errors obtained using the Ghosh equation are approximately 47 MPa (13%) at 50% true strain and 67 MPa (18%) at 60% true strain.

For the W-Temper process route the Ludwik-Hollomon, Ludwik-Hollomon-modified and Ghosh equations indicate the highest deviation values of 56–59 MPa (16–17%) at true strain values of 50% and 77–79 MPa (21–23%) at true strain values of 60%. Using the Hockett-Sherby equation the deviation between the measured and calculated flow stress is 1 MPa (0.4%) at a true strain of 50% and 3 MPa (0.8%) at a true strain of 60%. This corresponds well with the results from Schneider et al. [34] for EN AW-6016 material where the Ludwik-Hollomon and Ludwik-Hollomon-modified models approximated similar stress values and the Hockett-Sherby formulation showed the best correlation with the experimental data. For the Hotforming and W-Temper process routes it seems that the models considering dynamic recovery mechanisms during deformation [35] estimate the hardening behaviour with higher accuracy.

Considering the Warmforming process the flow stress values calculated using the Voce equation differ from the experimentally determined data by approximately 15 MPa (4%) at 30% true strain. The values determined using the Ludwik-Hollomon and Ludwik-Hollomon-modified equations differ by less than 1 MPa with the modified model

showing slightly reduced LSE values in the uniform elongation region (Table 3). Using the Hockett-Sherby model a deviation of 15 MPa (4%) is observed between the measured and calculated flow curves. The absolute stress value deviation obtained using the Ghosh equation is approximately 4 MPa (1%). Considering a relatively small area of uniform elongation in the stress-strain curve (Figure 5, dashed curve) the power law approximations seem to provide a high correlation with the experimentally determined support point. Future work has to clarify whether hybrid approximation models, such as the combination of Hockett-Sherby and Swift, result in a higher correlation with the experimental data. Further, the validity of future tests may be enhanced by comparing the entire flow curve of the layer compression test with the extrapolated data.

5 Conclusion

The prediction of plastic strains and flow stresses is a critical factor in sheet metal forming, especially in the context of heat-assisted forming processes of lightweight materials such as high-strength aluminium alloys. Although empirically based flow curve models approximate the flow behaviour within the uniform elongation region with reasonable accuracy, there are significant deviations when extrapolating to higher strain values. In this study the flow behaviour of

EN AW-7021 sheet material has been investigated for different forming processes using tensile and layer compression tests; the latter providing a support point to indicate the extrapolation quality of the approximate model.

The main conclusions of this study are as follows:

- For the Hotforming and W-Temper testing routes the experimentally obtained flow curves show a high correlation within the uniform elongation region which is assumed to be due to the same material condition.
- For the Warmforming temperature profile the experimentally obtained flow curve is mainly characterised by a negative strain hardening coefficient. Layer compression tests indicate the accuracy of the empirical models at higher strain values, despite the significantly lower uniform elongation region compared with the Hotforming or the W-Temper process route.
- In the region of uniform elongation the Ludwik-Hollomon, Ludwik-Hollomon-modified and the Ghosh equation indicate the highest LSE-values and thus the highest deviations from the experimental data. This applies to all heat-assisted process routes investigated.
- The Hockett-Sherby model shows the least deviation from the experimental data when considering the Hotforming ($\Delta\sigma < 20$ MPa) and W-Temper ($\Delta\sigma < 3$ MPa) temperature profiles in the range of extrapolated strain values. This indicates a high quality of extrapolation.
- Considering the Warmforming process route, all approximation models seem to estimate the flow behaviour with reasonable accuracy. However, the Ludwik-Hollomon-modified approximation model was found to show the best correlation with the experimental data indicating an absolute deviation of $\Delta\sigma < 1$ MPa. The Hockett-Sherby equation, which seems to be well suited to all temperature profiles, indicates an absolute deviation of $\Delta\sigma < 16$ MPa.

Declarations

Conflict of interest The authors declare that they have no conflict of interest.

References

1. Zhou B, Liu B, Zhang S (2021) The Advancement of 7XXX Series Aluminum Alloys for Aircraft Structures: A Review. Metals 11:718. https://doi.org/10.3390/met11050718
2. Schuster P, Österreicher J, Kirov G, Sommitsch C, Kessler O, Mukeli E (2019) Characterisation and Comparison of Process Chains for Producing Automotive Structural Parts from 7xxx Aluminium Sheets. Metals 9:305. https://doi.org/10.3390/met9030305
3. Zheng K, Politis DJ, Wang L, Lin J (2018) A review on forming techniques for manufacturing lightweight complex—shaped aluminium panel components. Int J Lightweight Mater Manuf 1:55–80
4. Liu Y, Zhu Z, Wang Z, Zhu B, Wang Y, Zhang Y (2017) Formability and lubrication of a B-pillar in hot stamping with 6061 and 7075 aluminum alloy sheets. Proced Eng 207:723–728
5. Behrens B-A, Hübner S, Vogt H, Golovko O, Behrens S, Nürnberger F (2020) Mechanical properties and formability of EN AW-7075 in cold forming processes. IOP Conf Ser. Mater Sci Eng 967:12017. https://doi.org/10.1088/1757-899X/967/1/012017
6. Polak S, Kaczyński P, Gronostajski Z, Jaskiewicz K, Krawczyk J, Skwarski M, Zwierzchowski M, Chorzępa W (2017) Warm forming of 7075 aluminum alloys. Proced Eng 207:2399–2404. https://doi.org/10.1016/j.proeng.2017.10.1015
7. Drotleff K (2021) Verbesserte Prognose lokaler Einschnürungen in mehrstufigen Blechumformprozessen. Dissertation, Universität Stuttgart. https://doi.org/10.18419/opus-11604
8. Zhuang X, Zhao Z, Li H, Xiang H (2013) Experimental Methodology for Obtaining the Flow Curve of Sheet Materials in a Wide Range of Strains. Steel Res Int 84:146–154. https://doi.org/10.1002/srin.201200104
9. DIN EN ISO 6892-1 (2020) Metallic materials - Tensile testing - Part 1: Method of test at room temperature. Beuth, Berlin
10. DIN EN ISO 16808 (2022) Metallic materials - Sheet and strip - Determination of BIAXIAL stress-strain curve by means of bulge test with optical measuring systems. Beuth, Berlin
11. Brosius A, Yin Q, Güner A, Tekkaya AE (2011) A New Shear Test for Sheet Metal Characterization. Steel Res Int 82:323–328. https://doi.org/10.1002/srin.201000163
12. DIN EN ISO 50106 (2023) Testing of metallic materials - Compression test at room temperature. Beuth, Berlin
13. Alves LM, Nielsen CV, Martins PAF (2011) Revisiting the Fundamentals and Capabilities of the Stack Compression Test. Exp Mech 51:1565–1572. https://doi.org/10.1007/s11340-011-9480-5
14. Merklein M, Kuppert A (2009) A method for the layer compression test considering the anisotropic material behavior. Int J Mater Form 2:483–486. https://doi.org/10.1007/s12289-009-0592-8
15. Albiez C, Liewald M, Görres A, Regensburger J (2011) Numerical prediction of thermal panel distortion incorporating thermal material properties of 6016 aluminum alloy. In: Gesamtverband der Aluminiumindustrie e.V. (ed) European Aluminium Congress
16. Gese H, Keller S, Yeliseyev V, Dell H (2007) Ermittlung von Fließwiderstandskurven bei großen Formänderungen für die Blechumformsimulation. In: Frenz H, Wehrstedt A (eds)

Kennwertermittlung für die Praxis: 20 Tagung Werkstoffprüfung 2002. Wiley-VCH, Weinheim, pp 242–249

17. Joun M, Eom JG, Lee MC (2008) A new method for acquiring true stress–strain curves over a large range of strains using a tensile test and finite element method. Mech Mater 40:586–593

18. Heine B (2015) Werkstoffprüfung: Ermittlung der Eigenschaften metallischer Werkstoffe, Hanser Verlag, München

19. Lohmar J, Bambach M, Hirt G (2014) Comparison of Semi-empirical and Dislocation Density based Material Equations for Fast Modeling of Multistage Hot Working of Steel. Proced Eng 81:268–273

20. Svyetlichnyy D, Nowak J, Mikhalyov A (2013) Flow Stress Model Based on Internal Variables. AMR 717:200–204. https://doi.org/10.4028/www.scientific.net/AMR.717.200

21. Doege E, Behrens B-A (2016) Handbuch Umformtechnik. Springer, Berlin Heidelberg

22. Birkert A, Haage S, Straub M (2013) Umformtechnische Herstellung komplexer Karosserieteile: Auslegung von Ziehanlagen. Springer, Berlin Heidelberg

23. Quetting F, Hora P, Roll K (2012) Modelling of Strain Hardening Behaviour of Sheet Metals for Stochastic Simulations. KEM 504–506:41–46

24. Ostermann F (2014) Anwendungstechnologie Aluminium. Springer, Berlin Heidelberg

25. Kahrimanidis A, Lechner M, Degner J, Wortberg D, Merklein M (2015) Process Design of Aluminum Tailor Heat Treated Blanks. Materials 8:8524–8538. https://doi.org/10.3390/ma8125476

26. Merklein M (2006) Charakterisierung von Blechwerkstoffen für den Leichtbau. Meisenbach, Bamberg

27. Hoffmann H (2012) Handbuch Umformen. Hanser Verlag, München

28. DIN 50125 (2022) Testing of metallic materials - Tensile test pieces. Beuth, Berlin

29. Milkereit B, Österreich M, Schuster P, Kirov G, Mukeli E, Kessler O (2018) Dissolution and Precipitation Behavior for Hot Forming of 7021 and 7075 Aluminum Alloys. Metals 8:531. https://doi.org/10.3390/met8070531

30. Schneider R, Heine B, Grant RJ, Zouaoui Z (2015) Mechanical behaviour of aircraft relevant aluminium wrought alloys at low temperatures. Proc IMechE 229:126–136. https://doi.org/10.1177/1464420713501734

31. Grohmann T (2016) Forming of AMAG 7xxx Series Aluminium Sheet Alloys, presented at New Developments in Sheet Metal Forming. Stuttgart

32. Lenzen M, Kraus M, Merklein M (2021) Analytical friction force compensation of flow curves out of layer compression tests with the pin extrusion test. Int J Mater Form 14:663–676

33. Hetz P, Lenzen M, Kraus M, Merklein M (2021) Determination of the Biaxial Anisotropy Coefficient Using a Single Layer Sheet Metal Compression Test. KEM 883:303–308. https://doi.org/10.4028/www.scientific.net/KEM.883.303

34. Schneider R, Grant RJ, Sotirov N, Falkinger G, Grabner F, Reichl C, Scheerer M, Heine B, Zouaoui Z (2015) Constitutive flow curve approximation of commercial aluminium alloys at low temperatures. Mater Design 88:659–666. https://doi.org/10.1016/j.matdes.2015.09.034

35. Kocks UF, Mecking H (2003) Physics and phenomenology of strain hardening: the FCC case. Progress Mater Sci 48:171–273